Full text open access online (Since 2001)

PRINT: ISSN 0972-3757 ONLINE: ISSN 2456-6330
Int J Hum Genet, 25(2): 59-66 (2025)
DOI: 10.31901/24566330.2025/25.02.909

# A Nonsense Mutation in *FBN1* Presented with Variable Phenotypes of Marfan Syndrome within a Chinese Family

**Jie Li[1], Yan Song[2], Zonghui Feng[3], Xueshuang Huang[4], Shengmei Yang[5], Yiling Yang[6], Bin Wang[7*] and Haiou Jiang[8*]**

*[1,2,4,5,6,8]Institute of Biomedicine, School of Basic Medicine, Hunan University of Medicine, Huaihua, China*
*[7]Key Technology Engineering Center for New Veterinary Vaccine and Industry of Yunnan Provincial Education Department, Kunming University, Kunming, Yunnan, China*
*[3]Department of Medical Genetics, Huaihua City Maternal and Child Health Care Hospital, Huaihua, China*

**KEYWORDS** *FBN1* Gene. Marfan Syndrome. Phenotype. Semi-dominant Inheritance. Variant

**ABSTRACT** Marfan syndrome (MFS) exhibits an irregular dominant connective tissue defect with clinical variability. It generally affects the skeletal, ocular, and cardiovascular systems. The variants in the *FBN1* gene are the main causes of this disease. In this study, Exome sequencing and Sanger sequencing were utilised to explore the pathogenic variant of a Chinese MFS family. A nonsense variant c.612C>A (C204X) of *FBN1* was identified in the both affected brothers with different clinical phenotypes and in their unaffected mother. Nevertheless, the variant was absent in 200 healthy controls. The further cell function experiment demonstrated that the FBN1 C204X mutant exhibited a lower level of mRNA and protein expression than the wild-type. The results supplemented the data of genotype-phenotype relationships in regard to *FBN1* variants, and expanded the *FBN1* variants spectrum in Asian populations. This study confirmed that MFS was a semidominant genetic disorder probably involving the special hereditary modifiers and environmental risk factors.

## INTRODUCTION

Marfan syndrome (MFS) presents with variable manifestations and genetic diversity, which is an autosomal dominant genetic defect of connective tissue. The morbidity rate is approximately 1:5000 individuals (Pyeritz 1993). Although the risk of alterable MFS is higher in cases with a kin history, the condition does not distinguish between different ethnicities and genders (Ramachandra et al. 2015). MFS mainly affects the ocular, skeletal and cardiovascular systems, and includes more than 30 different clinical presentations (Verstraeten et al. 2016). The main causes of mortality are aortic root dilatation and acute aortic dissection in MFS. The previous researches showed that 91 percent of MFS cases were caused by fibrillin-1 (*FBN1*) gene mutations (MFS-1, OMIM 134797) (Loeys et al. 2004), whereas a very small percentage of the patients were associated with *TGFBR2* gene (MFS-2, OMIM 190182) mutations (Waldmuller et al. 2007). Fibrillin-1 is a crucial element of connective tissues with a 350-kDa glycoprotein of extracellular microfibrils. It is encoded by the large *FBN1* gene on 15q21.1 (Sakai et al. 1986). The *FBN1* gene contains 66 exons spanning 235 kb of genomic DNA, which is broadly expressed in the ciliary zonules of the eye, tendons, periosteum, and aorta (Liu et al. 2021). It has been known that 6 fibrillin-1 monomers form an immense complex ectocytic aggregation, defined as a microfibre. This microfibre has a significant role for the integrality and stability of both inelastic and elastic tissues (Sakai et al. 1986; Pereira et al. 1997). Should the *FBN1* mutations result in the destruction of microfibril formation and function, it would cause an obstruction of the TGF-β signalling pathway (Le Goff et al. 2011), subsequently turning off the fibrillin-1 channel,

*Address for correspondence:*
Dr. Haiou Jiang
Institute of Biomedicine, Hunan University of Medicine, 492#, Jinxi South Road, Huaihua, Hunan 418000, China
*Telephone:* +86 745 2382903
*Fax:* +86 745 2382082
*E-mail:* hhjiangh@126.com

*Address for co-correspondence:*
Dr. Bin Wang
Key Technology Engineering Center for New Veterinary Vaccine and Industry of Yunnan Provincial Education Department, Kunming University,
2#, Puxin Road, Economic Development Area, Kunming, Yunnan650214, China.
*E-mail:* wangbbiomed@126.com

consequently, extensively hindering the function of the ocular, skeletal, and cardiovascular systems (Niu et al. 2020). Although over 3000 mutations within *FBN1* have been described to be responsible for MFS so far, the precise phenotype-genotype correlation remains indistinct owing to the heterogeneity of *FBN1* variation (Tian et al. 2024; Wu et al. 2020).

In the present research, a combination of Exome sequencing and Sanger sequencing was utilised to search for the causative variant of a Chinese pedigree with MFS. A heterozygous nonsense variant c.612C>A (C204X) in *FBN1* was detected. This variant produced a relatively lower level of *FBN1* mRNA and protein expression in the patients than in healthy individuals through nonsense-mediated mRNA decay (NMD), which probably resulted in MFS for the Chinese family.

### Objective

The objective of this study is to clarify the clinical phenotype of a Chinese family affected with MFS, and to elucidate its molecular etiology by genetic analysis and in vitro cell function experiment.

## METHODOLOGY

### Clinical Material

A Chinese MFS family with 2 affected members was recruited in this study (Fig.1). Subsequently, 6 related family members were subject to ophthalmic examinations, imaging examinations (echocardiography or computer tomography), systemic assessments incorporating skeletal inspections, health examinations, the skin extensibility and aortic root diameter detections. The family proband was first diagnosed with MFS based on the revised Ghent nosology.

### Ethics Statement

The present study complied with the Declaration of Helsinki, and all participants provided written informed consent. The experimental program was authorised by the Ethics Committee of Hunan University of Medicine.

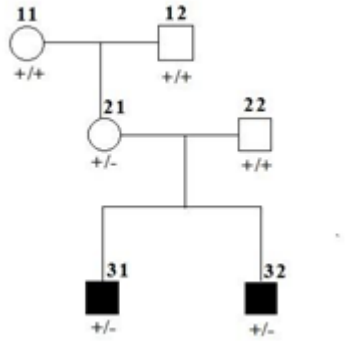


**Fig.1. Pedigree and genotypes of a three-generation Chinese family with FBN1 mutation. Affected individuals were indicated by solid squares (males) or circles (females). Normal individuals were indicated by open symbols. Arrow showed the proband. " and + meant the mutant and wild type alleles, respectively**

### Exome Sequencing

Peripheral blood samples were collected from two affected (31 and 32) and four unaffected individuals (11, 12, 21 and 22) for mutation identification. Genomic DNA (gDNA) was prepared from peripheral white blood cells of all participants according to the instructions of the manufacturer (Tiangen Biotech Co. Ltd., Beijing, China). Then, Exome sequencing was performed on the two patients (31 and 32) in the family by the SierraVast Biomedical Technology Co. Ltd. headquartered in Shanghai, China. Following the protocol of the manufacturer, the exome library was constructed using a minimum of 1.5 μg of gDNA for each sample. The eligible gDNA was randomly sheared into an average piece of 500 bp using sonication, and then the DNA library was enriched and hybridised for exons aggregation applying Agilent SureSelectXT Human All Exon V7 in accordance with the instructions of the manufacturer (Agilent Technologies Inc., Santa Clara, CA). Subsequently, the fragments that had been captured were subjected to amplification, purification and paired-end sequencing using Illumina Novaseq sequencer (Illumina, CA). The average sequencing depth was more than 100× for each sample. By using Fastx-tools, low quality reads were removed. The qualified data were mapped to the human reference assembly (hg19). The reads aligned to the target

and neighboring regions of the samples were gathered and merged into an "mpileup" file with SAM tools for succedent analyses. In the subsequent analysis, the variants were discarded incorporating single nucleotide variants (SNVs) and insertions/deletions (indels) in the sites of segmental repetitions and unallocated chromosomes. After excluding the repetitive reads and recalibrating the base quality scores, SNVs and indels were initially identified employing Haplotyper of Sentieon for both the samples. Afterwards, variant quality score recalibration and hard filter means were utilised in order to acquire the high-quality variant calls for SNVs and indels. The identified SNVs and indels were interpreted using SnpEff software, and online databases, namely, OMIM, HGMD, GnomAD, and ClinVar. Subsequently, the researchers performed a preferential screening for shared variants in *FBN1* and *TGFBR2* gene for the both samples. The pathopoiesis of variants was classified according to the guidelines established by the American College of Medical Genetics and Genomics (ACMG). It involved the following classifications of benign, likely benign, uncertain significance, likely pathogenic, and pathogenic.

**Mutation Verification**

After Exome sequencing, conventional Sanger sequencing was adopted to validate the alternative variants and ascertain whether they co-segregated with phenotype of the family. The primers of underlying pathogenic variants of *FBN1* gene (NM_000138) were designed with online Primer3 software (http://bioinfo.ut.ee/primer3/) and chemically synthesised by Genewiz Biotechnology Co. Ltd. The polymerase chain reaction (PCR) amplification was implemented in a 25 μL reaction mixture, comprising 1.0 μL of each of the forward and reverse primers, 50 ng of gDNA, and 12.5 μL of 2 × Taq Master Mix (Huiling Biotech Co. Ltd, Shanghai, China). Thermocycling was carried out in accordance with the following protocol, that is, an initial denaturation at 95°C for 5 minutes, subsequently running 35 cycles of denaturation at 95 °C for 30 seconds, annealing at 60 °C for 30 seconds, extending at 72 °C for 30 seconds, and eventually extending at 72 °C for 5 minutes. The amplicons were subjected to electrophoresis utilising 1.5 percent agarose gels, and subsequently purified using the CyclePure Kit (OMEGA; Bio-Tek, Doraville, GA). Sanger sequencing was bidirectionally carried out on an ABI PRISM 3730 sequencing instrument (Applied Biosystems). These data were blasted by an online website (https://blast. ncbi. nlm.nih.gov/). Additionally, 100 ethnicity-matched unrelated normal controls were also sequenced in the same way.

**Structure-based Model Building and Analysis**

Taking advantage of I-TASSER, an automated homology modelling procedure (http:// zhanglab.ccmb.med.umich.edu/), the researchers performed three dimensional (3D) modeling of Fibrillin-1 of the human wild-type and mutant. The wild-type protein consists of 2871 amino acids (NP 000129.3) and the mutant protein consists of 204 amino acids. Employing Swiss-Pdb Viewer 4.1 software, the researchers visualised data acquired from the homology models.

**Plasmid Construction**

Overexpression plasmid of human *FBN1* gene named pcDNA3.1-*FBN1*-3xFlag (G138369) was obtained commercially from Youbio Biotech Company (Changsha, China). The target gene fragment of FBN1 C204X was obtained by PCR, and then the pCDNA3.1-3xF1ag plasmid vector (VT9221) and the FBN1 C204X target gene fragment were enzymatically cleaved. Subsequently, the cleaved target gene fragment and vector backbone were homologously recombined. The recombination product was directly transformed and coated onto plates, and then clones were selected for positive mutant identification. All the sequences of the plasmid were sequenced and verified by HonorGene (Changsha, China).

**Western Blot Analysis**

The protein was isolated from cells using RIPA lysis buffer (YSD0100, Yoche) comprising protease inhibitor Cocktail (BL507A, biosharp). Afterwards, ultrasonic treatment was performed on the samples. Then the protein was quantified by the enzyme-labelled instrument (Tristar LB 942, Berthold). The selection of an SDS-PAGE gel with a concentration of 8 percent was deter-

mined by the molecular weight of the target protein. The precipitated proteins (20μg) were separated in Western Running Buffer by 120 V electrophoresis after constant pressure of 80 V for 40 minutes. Then the protein was transferred to the PVDF membrane in Western Transfer Buffer, with a constant current of 290 mA for 90 minutes. Furthermore, the transferred protein was sealed with 5 percent skim milk at ambient temperature for one hour, and subsequently it was incubated with the primary antibody (fibrillin-1 antibody, ABclonal, A16677, 1:1000; Actin antibody, Abbkine, KTD101-EN, 1:1000) at 4 overnight. Once more it was incubated with the secondary antibody (Goat anti-Rabbit/Mouse IgG(H+L) HRP, Abways, AB01, 1:10000) at ambient temperature for one hour. Finally, the bands of protein were fully reacted with ECL chromogenic solution and inspected using enhanced chemiluminescence (ChemiDoc MP Imaging System, Bio-Rad).

### qPCR

The total RNA of cells was extracted using an RNA extraction kit (Beyotime, R0077S). Then, reverse transcription was carried out to produce cDNA using a cDNA reverse-transcription kit (Jingke biology, TSK322S). Subsequently, the qPCR reaction was performed using the SYBR Green Fast qPCR Mix (2×) kit (ABclonal, RM21203). qPCR reaction system was detected by CFX96 Real-Time PCR Detection System (Roche, LightCycler 480). Primers for target gene *FBN1* and housekeeping gene ACTIN were designed with online Primer3 software (http://bioinfo.ut.ee/primer3/), and then synthesised by Jingke Biotechnology Company. Primer sequences was as follows. *FBN1* Forward Primer: GTGACTGCCCACCTGATTTT; *FBN1* Reverse Primer: CAGCAGGAAGCTTTGGAAAC; ACTIN Forward Primer: GGCATGGGTCAGAAGGATT; ACTIN Reverse Primer: TGGTGCCAGATTTTCTCCA. The PCR procedure was as follows, that is, 2 minutes at 50°C, then 10 minutes at 95°C, followed by 15 seconds at 95°C and a further 1 minute at 60°C with a total of 40 cycles. The gene expression of the relative amount mRNA was analysed based on ΔΔCT.

## RESULTS

### Clinical Manifestation

The proband (31) was a 23-year-old male with a height of 181 cm. The length of his legs and arms were 90 cm and 74 cm, respectively. His fingers and toes were also long and thin with spidery-like shapes. His chest also showed a caved-in look, and his spine presented scoliosis. His entire body displayed the skin striae. Electrocardiogram examination for him demonstrated sinus rhythm and no symptom of ischemic alterations. Echocardiography detection showed an aortic root dilation with a diameter of 44 mm and mitral valve prolapse. Computed Tomography (CT) scan exhibited a type A aortic dissection (Fig. 2) for the ascending and descending aorta. The proband was clinically diagnosed with typical Marfan syndrome without ectopia lentis. His old brother (32), a 27-year-old male, was mainly characterised by positive 'thumb signs' and 'wrist signs', overgrowth of the long bones, Pectus Excavatum, skin striae, and pneumothorax, but he was not associated with dilative aortic root, mitral valve prolapse and aortic dissection at present. Other normal relatives were absent of positive phenotype of MFS in the family. Detailed clinical data of two affected individuals and their parents were listed in Table 1. The intra-familial phenotypic heterogeneity of MFS was observed in the Chinese family.

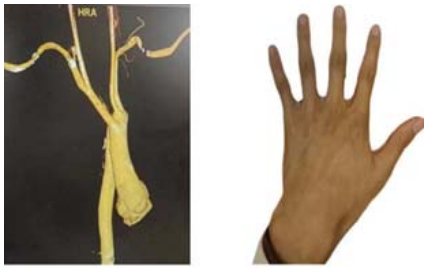


**Fig.2. Clinical characteristics of MFS family. (a) Computed tomography scan showed the type A aortic dissection of the proband (32). (b) The proband's old brother (31) exhibited spidery-likefingers**

### Exome Sequencing

Total 22.64 Gb data were acquired from the two sequenced patients. The mean depth of the two samples was 160× and 162.6×, respectively. Furthermore, the target exome coverage of each sample exceeded 99 percent. The capture rate for both 31 and 32 samples was found to be up to 92.62 percent and 88.86 percent, respectively.

**Table 1: Clinical information of the family members**

| *Characteristic* | *Proband (31)* | *Proband's elder brother (32)* | *Proband's mother (21)* | *Proband's father (22)* |
|---|---|---|---|---|
| Gender | M | M | F | M |
| Wrist and thumb sign | + | + | - | - |
| Pectus Excavatum | + | + | - | - |
| Plain Flat Foot | - | - | - | - |
| Facial features | | | | |
| Myopia | - | - | - | - |
| Lens dislocation | - | - | - | - |
| Overgrowth of the long bones | + | + | - | - |
| Aortic dissection | - | - | - | - |
| Dilatation of the ascending aorta | + | - | - | - |
| Pneumothorax | - | + | - | - |
| Mitral regurgitation | + | - | - | - |
| Scoliosis | + | - | - | - |
| Skin striae | + | + | - | - |

After all qualified raw reads were blasted to the human reference genome, the researchers initially eliminated synonymous variants and known frequent variants reported in dbSNP137, 1000 Genomes data, HapMap8, and the YH1 project. No causative variant was found in *TGFBR2* gene in relation to MFS. However, within the known pathogenic *FBN1* gene, a rare heterozygous variant c.612C>A (C204X) in exon 6 was identified in the both patients. The variant was hypothesised to hinder the function of *FBN1* by means of a known NMD mechanism. This led to a reduction in gene expression and a disruption in protein function, which possibly resulted in the occurrence of MFS. According to the standards and guidelines of ACMG, the variant was deemed to likely be pathogenic. Simultaneously, it was classified as PVS1 and PM2.

## Validation of Pathogenic Mutations

The heterozygous variant c.612C>AC204X of *FBN1* (Fig. 3) was observed in the both affected patients and their unaffected mother utilising Sanger sequencing, and was not present in the other 3 normal family individuals and 100 ethnicity-matched unrelated healthy members. This variant converted the 204$^{th}$ cysteine residues into a stop codon, creating a truncated protein. The variant was closely related to phenotypes of the Chinese pedigree. The fairly complex phenotype of the variant was a remarkable

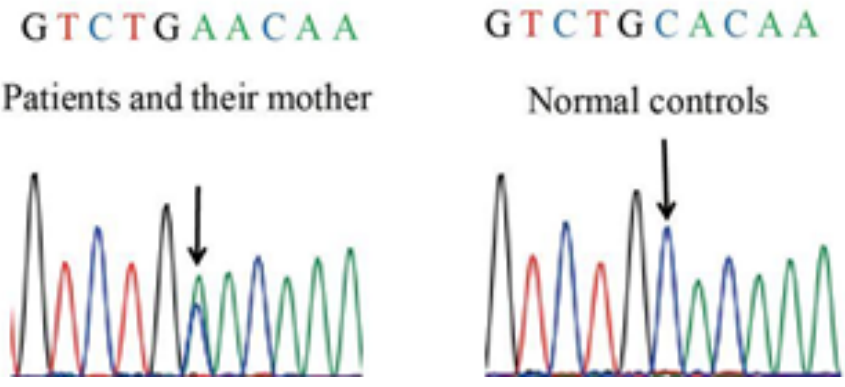


**Fig. 3. Sanger sequencing of the FBN1 gene. The heterozygous c.612C>A variation was found in the two patients (31, 32) and their mother (21), not in the other normal controls (11, 12, 22). The arrow indicated the mutated site**

manifestation in the family and there might also be hereditary and/or environmental risk factors affecting the mutant phenotype of *FBN1*.

### Structural Modelling

A three-dimensional molecular model of fibrillin-1 was built to analyse the structure of WT/Mut proteins. It was used to predict the mutant pathogenic role on the basis of the crystal structure (Fig. 4). The constructed models of WT/Mut proteins matched the target sequence of fibrillin-1 (WT residues 1-2871, Mut residues 1-204). In the light of the model, there existed a 50 percent sequence identity between WT *FBN1* and its target template. The wild and mutant structure of fibrillin-1 was analysed utilising Swiss-Pdb Viewer 4.1 software. The researchers discovered that the mutant fibrillin-1 structure was incomplete compared with the wild-type protein structure.

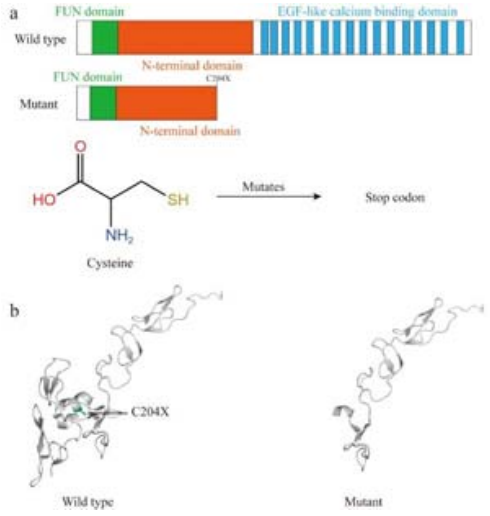


**Fig. 4. Protein structural analysis of c.612C>A variant. (a) The schematic diagram of FBN1 protein indicated the loss of entire cb-EGF domains in mutant. (b) The 3D molecular models revealed the incomplete structure of mutant-type protein**

### Functional Validation of the Wide-type and Mutant of *FBN1*

In vitro experimentation revealed a substantial decrease in the mRNA and Protein expression of fibrillin-1 in mutated cells, as compared with the control group (Fig. 5). It suggested that the mutant of *FBN1* was pathogenic, which may result in the dysfunction of normal protein function and the occurrence of MFS.

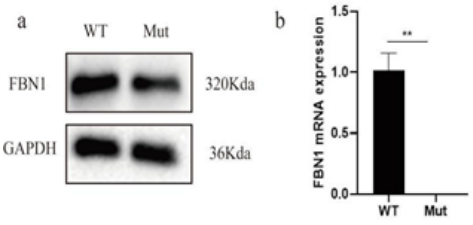


**Fig. 5. The dysfuction of FBN1 mutant protein. (a) The decreased expression of the FBN1 mutant protein. (b)The decreased expression of the FBN1 mutant mRNA**

## DISCUSSION

Marfan syndrome is accompanied by intricate clinical presentations of multiple organ systems, commonly involving the skeletal, ocular, and cardiovascular systems. Clinically, aortic root aneurysm and aortic dissection for MFS are the most mortal and outstanding signs (Biggin et al. 2004). *FBN1* gene was confirmed to be responsible for MFS in 1991 (Dietz et al. 1991). The profibrillin-1 encoded by *FBN1* can be processed to fibrillin-1 as the major ingredient of extracellular microfibrils (Ramirez and Sakai 2010). The modular structure of fibrillin-1 mainly involves seven TB domains (transforming-growth-factor-β1-binding protein), and 47 EGF domains (epidermal-growth-factor) among which 43 are cb-EGF domains (calcium binding) (Handford 2000). Each EGF domain consists of six extremely conservative cysteine residues, which creates the tertiary structure of the protein by forming disulfide bonds (Niu et al. 2020). There are two main sorts of *FBN1* genetic mutations that can potentially influence the fibrillin-1 structure, that is, nonsense and missense mutations. In addition, several splice-site mutations, in-frame deletions and insertions, and large genomic rearrangements have also been identified (Buki et al. 2023). As demonstrated in the study by Tan et al. (2017), variants of *FBN1* not only lead to representative MFS, but also significantly impact on the etiologic mechanism of sporadic cas-

es. Even in the same family, the different family individuals with the same *FBN1* variant showed very different clinical presentation, including the variability in tissue distribution, onset age and severity of MFS (Robinson et al. 2002). Previous studies demonstrated that the allelic variant may not be the sole factor affecting the MFS clinical feature (Zhao et al. 2013).

In the present study, a nonsense variant c.612C>A (C204X) of the *FBN1* gene was identified applying Exome sequencing and Sanger sequencing. This variant transformed the 204$^{th}$ amino acid, a cysteine residues, into a stop codon, thereby creating a truncated protein. The foregoing researches have revealed that the majority of premature stop codon mutations of *FBN1* gene played a pivotal role in the molecular mechanism of MFS (Caputi et al. 2002), which resulted in a substantial reduction in the expression level of *FBN1* gene through NMD process (Culbertson 1999; Carrard and Lejeune 2023). In the current in vitro cell experiment, the expression of fibrillin-1 and the *FBN1* mRNA content coincided with the previous studies. This C204X variant would not only decrease the production of fibrillin-1 protein, but also lose the entire cbEGF domains of the protein. The researchers speculated that the truncated fibrillin-1 monomers could hamper the combination of normal monomers into extracellular microfibrils (Schrijver et al. 2002), and it resulted in the dysregulation of TGF-β signaling (Le Goff et al. 2011), subsequently blocking the fibrillin-1 channel, widely obstructing the function of the ocular, skeletal and cardiovascular systems, eventually giving rise to various clinical characteristics in MFS (Niu et al. 2020). But interestingly, the mutant in the Chinese family showed three quite different phenotypes with a genetic nonpenetrance pattern, including one patient of aortic dissection, one patient of skeletal deformity and one unaffected. The nonsense mutation had solely been described in a single MFS case of Arab ethnicity (Baudhuin et al. 2015), whose clinical features being akin to the proband of the Chinese family mainly involved cardiovascular lesion, aortic root dilation and skeletal deformity. The intrafamilial variability presented in the Chinese MF family also revealed that the allelic variant was not the exclusive determinant of clinical syndrome. Moreover, there might also be environmental factors and other specific genetic modifiers affecting the expression of a certain variant.

## CONCLUSION

In a word, the results supplemented the data of genotype-phenotype correlation with respect to *FBN1* variants. To the researchers' best current knowledge, they initially reported that the *FBN1* variant, c. c.612C>A (C204X), was observed simultaneously in three different main phenotypes (aortic dissection, skeletal deformity and unaffected) in the same Chinese family with MFS. Nonpenetrance of C204X carriers within *FBN1* gene was described for the first time in the Chinese family. This study supports that MFS is a semidominant genetic disorder involving hereditary and/or environmental risk factors.

## RECOMMENDATIONS

Collection of more cases is needed to thoroughly explain the association of *FBN1* mutations with clinical phenotype of MFS, because each sort of mutational occurrence is represented in a semblable proportion as in reference databases. Moreover, the potential environmental risk factors, or other modifier genes interacting with *FBN1* gene causing semidominant inheritance of MFS require further study.

## ACKNOWLEDGEMENTS

The researchers greatly thank the patients and their family members for their participation in this study. The work was sustained by the Pilot and Innovative Program for College Students in Hunan Province Education Department (No.202412214013, 202212214008, and 202312214012), and the Natural Science Foundation of Hunan Province (No.2025 JJ70427).

## AUTHORS' CONTRIBUTIONS

Jie Li and Yan Song contributed equally to this study. Study design and administrative support were by Haiou Jiang and Bin Wang, experiments design and data analysis and interpretation were by Jie Li, Yan Song, Haiou Jiang and Bin Wang, data collection was by Zonghui Feng, Xueshuang Huang, Shengmei Yang and Yiling Yang, and manuscript writing (drafting and revision) was by Jie Li and Haiou Jiang.

## REFERENCES


Baudhuin LM, Kotzer KE, Lagerstedt SA 2015. Decreased frequency of *FBN1* missense variants in Ghent criteria-positive Marfan syndrome and characterization of novel *FBN1* variants. *J Hum Genet,* 60(5): 241-252.

Biggin A, Holman K, Brett M et al. 2004. Detection of thirty novel *FBN1* mutations in patients with Marfan syndrome or a related fibrillinopathy. *Hum Mutat,* 23(1): 99.

Buki G, Szalai R, Pinter A et al. 2023. Correlation between large FBN1 deletions and severe cardiovascular phenotype in Marfan syndrome: Analysis of two novel cases and analytical review of the literature. *Mol Genet Genomic Med,* 11(7): e2166.

Caputi M, Kendzior Jr RJ, Beemon KL 2002. A nonsense mutation in the ffbrillin-1 gene of a Marfan syndrome patient induces NMD and disrupts an exonic splicing enhancer. *Genes Dev,* 16(14): 1754-1759.

Carrard J, Lejeune F 2023. Nonsense-mediated mRNA decay, a simplified view of a complex mechanism. *BMB Rep,* 56(12): 625-632.

Culbertson MR 1999. RNA surveillance: Unforeseen consequences for gene expression. inherited genetic disorders and cancer. *Trends Genet,* 15(2): 74-80.

Dietz HC, Cutting GR, Pyeritz RE et al. 1991. Marfan syndrome caused by a recurrent de novo missense mutation in the fibrillin gene. *Natur,* 352(6333): 337-339.

Handford P 2000. Fibrillin-1, a calcium binding protein of extracellular matrix. Biochimica et Biophysica Acta (BBA)-molecular. *Cell Res,* 1498(2-3): 84-90.

Le Goff C, Mahaut C, Wang LW et al. 2011. Mutations in the TGFbeta bindingprotein-like domain 5 of *FBN1* are responsible for acromicric and geleophysic dysplasias. *Am J Hum Genet,* 89(1): 7-14.

Liu W, Guo R, Hao H et al. 2021. Identification of a novel RHO heterozygous nonsense mutation in a Chinese family with autosomal dominant retinitis pigmentosa. *BMC Ophthalmol,* 21(1): 360.

Loeys B, De Backer J, Van Acker P et al. 2004. Comprehensive molecular screening of the *FBN1* gene favors locus homogeneity of classical Marfan syndrome. *Hum Mutat,* 24(2): 140-146.

Niu YP, Huang SX, Wang ZY et al. 2020. A nonsense variant in *FBN1* caused autosomal dominant Marfan syndrome in a Chinese family: A case report. *BMC Med Genet,* 21(1): 211.

Pereira L, Andrikopoulos K, Tian J et al. 1997. Targetting of the gene encoding fibrillin-1 recapitulates the vascular aspect of Marfan syndrome. *Nat Genet,* 17(2): 218.

Pyeritz R 1993. Marfan syndrome: Current and future clinical and genetic management of cardiovascular manifestations. *Semin Thorac Cardiovasc Surg,* 5(1): 11-16.

Ramachandra CJ, Mehta A, Guo KW et al. 2015. Molecular pathogenesis of Marfan syndrome. *Int J Cardiol,* 187: 585-591.

Ramirez F, Sakai LY 2010. Biogenesis and function of fibrillin assemblies. *Cell Tissue Res,* 339(1): 71-82.

Robinson PN, Booms P, Katzke S et al. 2002. Mutations of *FBN1* and genotype-phenotype correlations in Marfan syndrome and related fibrillinopathies. *Hum Mutat,* 20(3): 153-161.

Sakai LY, Keene DR, Engvall E 1986. Fibrillin, a new 350-kD glycoprotein, is a component of extracellular microfibrils. *J Cell Biol,* 103(6): 2499-2509.

Schrijver I, Liu W, Odom R et al. 2002. Premature termination mutations in *FBN1*: Distinct effects on differential allelic expression and on protein and clinical phenotypes. *Am J Hum Genet,* 71(2): 223-237.

Tan L, Li Z, Zhou C et al. 2017. *FBN1* mutations largely contribute to sporadic non-syndromic aortic dissection. *Hum Mol Genet,* 26(24): 4814-4822.

Tian F, Dong X, Yuan R et al. 2024. Case Report: Two different acromelic dysplasia phenotypes in a Chinese family caused by a missense mutation in FBN1 and a literature review. *Front Pediatr,* 12: 1428513.

Verstraeten A, Alaerts M, Van Laer L et al. 2016. Marfan Syndrome and related disorders: 25 years of gene discovery. *Hum Mutat,* 37(6): 524-531.

Waldmuller S, Muller M, Warnecke H et al. 2007. Genetic testing in patients with aortic aneurysms/dissections: A novel genotype/phenotype correlation? *Eur J Cardiothorac Surg,* 31(6): 970-975.

Wu Y, Sun H, Wang J et al. 2020. Marfan syndrome: whole-exome sequencing reveals de novo mutations, second gene and genotype-phenotype correlations in the Chinese population. *Biosci Rep,* 40(12): BSR20203356.

Zhao F, Pan X, Zhao K et al. 2013. Two novel mutations of ffbrillin-1 gene correlate with different phenotypes of Marfan syndrome in Chinese families. *Mol Vis,* 19: 751-758.


**Paper received for publication in January, 2025**
**Paper accepted for publication in June, 2025**